

# First Discovery of Tetravalent $\text{Ti}^{4+}$ Ion Conduction in a Solid

Naoyoshi Nunotani, Shinji Tamura, and Nobuhito Imanaka\*

Department of Applied Chemistry, Faculty of Engineering,  
Osaka University, 2-1 Yamadaoka, Suita,  
Osaka 565-0871, Japan

Received November 25, 2008

Revised Manuscript Received January 19, 2009

Solid electrolytes are unique functional materials in which only single ion species can generally migrate in the solid as a charge carrier, and some have already been commercialized as components of batteries and chemical sensing devices.<sup>1,2</sup> Although a large number of solid electrolytes have been found to obtain high ion conductivity that enters into the practical application range, such high ion conductivity is realized only for solids whose conducting species are mono-, di-, and trivalent ions. The high-valence tetravalent cation has been regarded as an extremely poor migrating species in solids because of strong electrostatic interaction between the tetravalent cation and surrounding anions, which prevents smooth ionic conduction in the solid lattice. To realize tetravalent cation conduction in solids, it is necessary to strictly select not only the crystal structure but also the constituent ions, in order to reduce such strong interactions. One of the most effective ways is the introduction of the cations with higher valence than the tetravalent ion into the structure, because such higher valence cations may attract anionic species more strongly than the tetravalent cation, enabling tetravalent cation migration in the solid lattice.

Recently, the tetravalent  $\text{Zr}^{4+}$  ion conducting  $\text{ZrM}(\text{PO}_4)_3$  ( $\text{M} = \text{Nb}, \text{Ta}$ )<sup>3,4</sup> and  $\text{Hf}^{4+}$  ion conducting  $\text{HfNb}(\text{PO}_4)_3$ <sup>5</sup> were successfully developed based on this concept. These solids contain two kinds of pentavalent  $\text{M}^{5+}$  ( $\text{M} = \text{Nb}, \text{Ta}$ ) and  $\text{P}^{5+}$  and possess the NASICON ( $\text{Na}^+$  super ionic conductor)-type structure having a three-dimensional network, which is well-known as a suitable structure for ion migration, with various kinds of NASICON-type solid electrolytes that conduct divalent<sup>6–8</sup> and trivalent<sup>9–11</sup> cations having been developed. Furthermore, the enhancement of  $\text{Zr}^{4+}$  ion

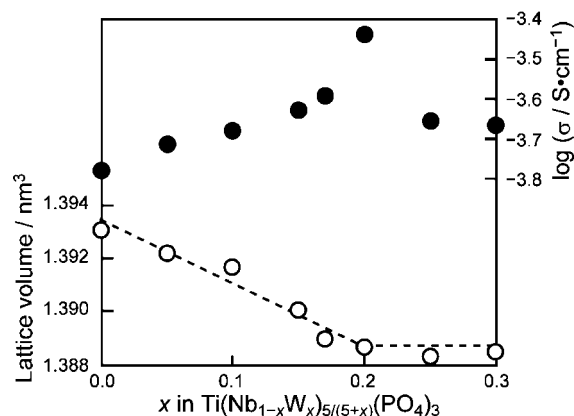


**Figure 1.** Compositional dependency of the lattice volume (○) and the electrical conductivity at 800 °C (●) for  $\text{Ti}(\text{Nb}_{1-x}\text{W}_x)_{5/(5+x)}(\text{PO}_4)_3$  solids.

conductivity for the  $\text{Zr}_{39/40}\text{TaP}_{2.9}\text{W}_{0.1}\text{O}_{12}$  solid,<sup>12</sup> which contains three high-valence cations of  $\text{Ta}^{5+}$ ,  $\text{P}^{5+}$ , and  $\text{W}^{6+}$  has also been demonstrated. However, the tetravalent cation species expected to conduct in these solids were limited to  $\text{Zr}^{4+}$  and  $\text{Hf}^{4+}$ , and the conduction of other tetravalent cations have not been reported.

In this communication, we report the conduction of the tetravalent  $\text{Ti}^{4+}$  ion in a solid. NASICON-type  $\text{TiNb}(\text{PO}_4)_3$  was selected as the mother solid, similar to the case for  $\text{Zr}^{4+}$  and  $\text{Hf}^{4+}$  ion conductors, and  $\text{W}^{6+}$  was partially substituted onto the  $\text{Nb}^{5+}$  site in an attempt to obtain high  $\text{Ti}^{4+}$  ion conductivity by reduction of the strong electrostatic interaction between the  $\text{Ti}^{4+}$  cation and the surrounding counter  $\text{O}^{2-}$  anions. The  $\text{Ti}^{4+}$  ion conducting properties of  $\text{Ti}(\text{Nb}_{1-x}\text{W}_x)_{5/(5+x)}(\text{PO}_4)_3$  were then investigated.

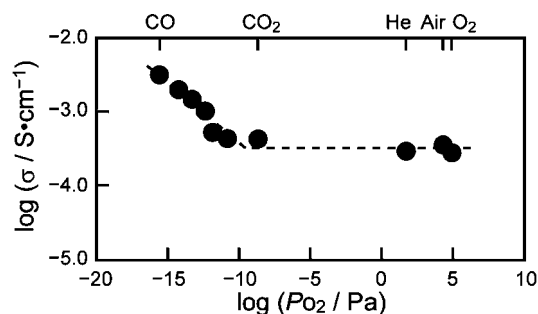
From X-ray diffraction (XRD) measurements of the  $\text{Ti}(\text{Nb}_{1-x}\text{W}_x)_{5/(5+x)}(\text{PO}_4)_3$  solids prepared, it was found that the single-phase rhombohedral ( $R\bar{3}c$ ) NASICON-type structure was obtained for the samples with  $x \leq 0.2$  (see Figure S1 in the Supporting Information). Furthermore, linear lattice shrinkage of the NASICON-type phase was observed with increasing W content ( $x$ ), as shown in Figure 1. In contrast, the samples with  $x > 0.2$  were multiphase mixtures of the NASICON-type solid,  $\text{TiP}_2\text{O}_7$  and  $\text{WO}_3$  without any lattice shrinkage of the NASICON-type phase compared to that with  $x = 0.2$ . This indicates that the smaller  $\text{W}^{6+}$  (ionic radius = 0.074 nm [coordination number (CN) = 6]<sup>13</sup>) ion successfully replaces  $\text{Nb}^{5+}$  (0.078 nm [CN = 6]<sup>13</sup>) in  $\text{TiNb}(\text{PO}_4)_3$  for samples with  $x \leq 0.2$ , and the solid solution limit composition of  $\text{Ti}(\text{Nb}_{1-x}\text{W}_x)_{5/(5+x)}(\text{PO}_4)_3$  for the single phase NASICON-type structure was identified to be around  $x = 0.2$ .

Figure 1 also presents the electrical conductivity of the  $\text{Ti}(\text{Nb}_{1-x}\text{W}_x)_{5/(5+x)}(\text{PO}_4)_3$  solids at 800 °C. The conductivity increased with the W content up to  $x = 0.2$ , the composition limit for the single-phase solid solution, to the highest

\* Corresponding author. E-mail: imanaka@chem.eng.osaka-u.ac.jp.

- (1) Yamamoto, O. *Solid State Electrochemistry*; Bruce, P. G., Ed.; Cambridge University Press: Cambridge, U.K., 1995; Chapter 11, pp 292–332.
- (2) Nagata, K.; Goto, K. S. *Solid State Ionics* **1983**, 9, 1249–1256.
- (3) Imanaka, N.; Ueda, T.; Adachi, G. *Chem. Lett.* **2001**, 30, 446–447.
- (4) Imanaka, N.; Ueda, T.; Adachi, G. *J. Solid State Electrochem.* **2003**, 7, 239–243.
- (5) Imanaka, N.; Itaya, M.; Adachi, G. *Mater. Lett.* **2002**, 53, 1–5.
- (6) Ikeda, S.; Takahashi, M.; Ishikawa, J.; Ito, K. *Solid State Ionics* **1987**, 23, 125–129.
- (7) Imanaka, N.; Okazaki, Y.; Adachi, G. *J. Mater. Chem.* **2000**, 10, 1431–1435.
- (8) Rambabu, G.; Rao, K. K.; Anantharamulu, N.; Raghavender, M.; Prasad, G.; Kumar, V. P.; Reddy, C. V.; Vithal, M. *J. Mater. Sci.* **2007**, 42, 3613–3620.
- (9) Tamura, S.; Imanaka, N.; Adachi, G. *Adv. Mater.* **1999**, 11, 1521–1523.

- (10) Hasegawa, Y.; Imanaka, N. *Solid State Ionics* **2005**, 176, 2499–2503.
- (11) Hasegawa, Y.; Hoshiyama, T.; Tamura, S.; Imanaka, N. *J. New Mater. Electrochem. Syst.* **2007**, 10, 177–180.
- (12) Imanaka, N.; Tamura, S.; Itano, T. *J. Am. Chem. Soc.* **2007**, 129, 5338–5339.
- (13) Shanon, R. D. *Acta Crystallogr., Sect. A* **1976**, 32, 751–767.



**Figure 2.** Relationship between the AC conductivity and the oxygen partial pressure at 800 °C.

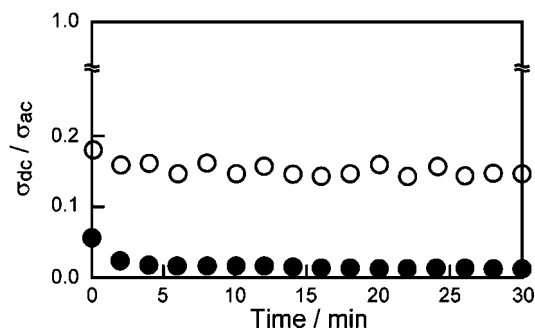


**Figure 3.** Time dependency of the DC to AC conductivity ratio ( $\sigma_{DC}/\sigma_{AC}$ ) for the  $\text{Ti}(\text{Nb}_{0.8}\text{W}_{0.2})_{5.0/5.2}(\text{PO}_4)_3$  solid in  $\text{O}_2$  ( $P_{\text{O}_2} = 1 \times 10^5$  Pa) (●) and  $\text{CO-CO}_2$  mixture ( $P_{\text{O}_2} = 1 \times 10^{-13}$  Pa) (○) atmospheres at 800 °C.

conductivity of  $3.65 \times 10^{-4} \text{ S cm}^{-1}$ . In the multiphase mixture region ( $x > 0.2$ ), the conductivity decreased because of the appearance of impurity phases of  $\text{TiP}_2\text{O}_7$  and  $\text{WO}_3$ .

For the purpose of identifying the conducting species in the  $\text{Ti}(\text{Nb}_{0.8}\text{W}_{0.2})_{5.0/5.2}(\text{PO}_4)_3$  solid, which exhibited the highest conductivity among the samples prepared, the oxygen partial pressure dependence of the AC conductivity was investigated at 800 °C (Figure 2). In the  $P_{\text{O}_2}$  range between  $1 \times 10^{-11}$  and  $1 \times 10^5$  Pa, the AC conductivities had a constant value independent of the oxygen pressure change, whereas the AC conductivity significantly increased with lowering of  $P_{\text{O}_2}$  below  $1 \times 10^{-11}$  Pa because of the appearance of electronic conduction caused by the reduction of  $\text{Ti}^{4+}$ . The constant AC conductivity in a wide oxygen partial pressure range clearly indicates that the predominant migrating species is an ion without any valence change. The polarization behavior was also investigated by measuring the time-dependent DC to AC conductivity ratio ( $\sigma_{DC}/\sigma_{AC}$ ) in oxygen ( $P_{\text{O}_2} = 1 \times 10^5$  Pa) and a  $\text{CO-CO}_2$  gas mixture ( $1 \times 10^{-13}$  Pa) at 800 °C and the results are presented in Figure 3. This procedure can provide information regarding the type of charge carrier in the solid.<sup>14</sup> In low  $P_{\text{O}_2}$  atmospheres (in this case, a  $\text{CO-CO}_2$  mixture), high DC conductivity was obtained because of the appearance of electronic conduction. In the case of the oxygen atmosphere, the  $\sigma_{DC}/\sigma_{AC}$  ratio abruptly decreased and reached values less than 0.013 after 30 min, suggesting that no electronic species was conducted in the  $\text{Ti}(\text{Nb}_{0.8}\text{W}_{0.2})_{5.0/5.2}(\text{PO}_4)_3$  solid. Polarization behavior in an oxygen atmosphere where sufficient  $\text{O}^{2-}$  can be supplied to the sample strongly indicates that  $\text{O}^{2-}$  ions do not migrate

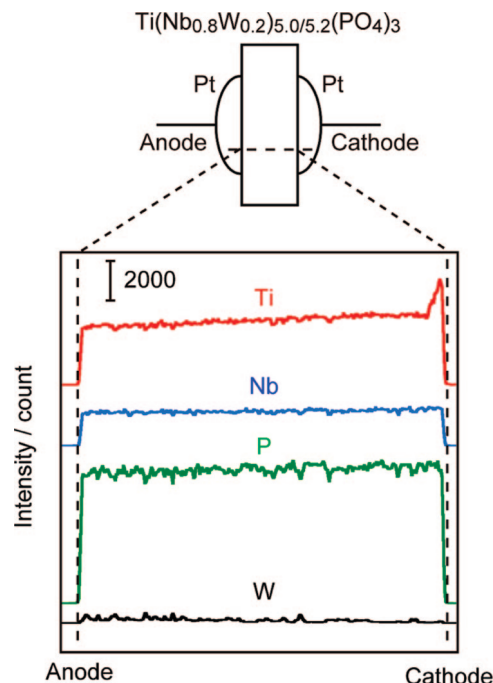


**Figure 4.** Experimental setup for DC electrolysis and EPMA line measurement results for the  $\text{Ti}(\text{Nb}_{0.8}\text{W}_{0.2})_{5.0/5.2}(\text{PO}_4)_3$  solid electrolyzed at 800 °C for 360 h.

in the sample. From these phenomena, it was clear that the conducting species in the  $\text{Ti}(\text{Nb}_{0.8}\text{W}_{0.2})_{5.0/5.2}(\text{PO}_4)_3$  solid is limited to cation species such as  $\text{Ti}^{4+}$ ,  $\text{Nb}^{5+}$ ,  $\text{P}^{5+}$  and  $\text{W}^{6+}$  in the  $P_{\text{O}_2}$  range higher than  $1 \times 10^{-11}$  Pa.

To directly demonstrate  $\text{Ti}^{4+}$  ion conduction in the  $\text{Ti}(\text{Nb}_{0.8}\text{W}_{0.2})_{5.0/5.2}(\text{PO}_4)_3$  solid, DC electrolysis was carried out by application of 4 VDC for 360 h at 800 °C. From preliminary investigation of  $I-V$  relationship, the decomposition voltage of the  $\text{Ti}(\text{Nb}_{0.8}\text{W}_{0.2})_{5.0/5.2}(\text{PO}_4)_3$  solid was determined to be ca. 1.2 V. By applying a DC voltage higher than the decomposition voltage, only the conducting cation species is forced to continuously and macroscopically migrate toward the cathode according to the potential gradient, and as a result, evidence of which cation species is migrating in the sample can be obtained by investigating the elemental distribution at or near the cathodic surface. After the DC electrolysis, electron probe microanalysis (EPMA) line analysis measurements of the electrolyzed pellet were performed, and clear segregation of only Ti near the cathodic surface was observed, as depicted in Figure 4, whereas other cations were distributed homogeneously over the sample. This result explicitly demonstrates the fact that tetravalent  $\text{Ti}^{4+}$  ions migrate in the  $\text{Ti}(\text{Nb}_{0.8}\text{W}_{0.2})_{5.0/5.2}(\text{PO}_4)_3$  bulk and deposit on the cathodic surface of the electrolyzed sample by application of a DC voltage.

The temperature dependency of the tetravalent ionic conductivity for  $\text{Ti}(\text{Nb}_{0.8}\text{W}_{0.2})_{5.0/5.2}(\text{PO}_4)_3$  is presented in Figure 5 with the corresponding data for  $\text{TiNb}(\text{PO}_4)_3$  ( $\text{Ti}^{4+}$  ion conduction was also demonstrated in this work. (see the Supporting Information)),  $\text{ZrNb}(\text{PO}_4)_3$ , and  $\text{HfNb}(\text{PO}_4)_3$ . The activation energy ( $E_a$ ), lattice volume, and the relative volume ratio of the tetravalent cation to lattice volume ( $A$  ratio =  $V_{\text{ion}}/V_{\text{lattice}}$ ) are also listed in Table 1. For  $\text{ZrNb}(\text{PO}_4)_3$  and  $\text{HfNb}(\text{PO}_4)_3$  with the same lattice volumes, the activation

(14) Imanaka, N.; Kobayashi, Y.; Adachi, G. *Chem. Lett.* **1995**, 24, 433–434.

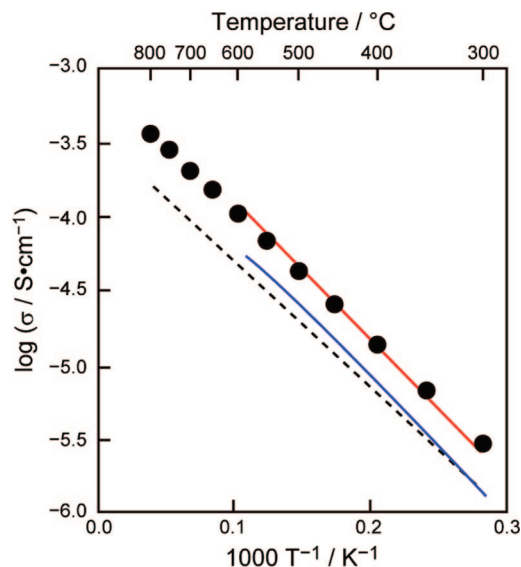


**Figure 5.** Temperature dependencies of tetraivalent cation conductivity for  $\text{Ti}(\text{Nb}_{1-x}\text{W}_x)_{5/5+x}(\text{PO}_4)_3$  (closed circle),  $\text{TiNb}(\text{PO}_4)_3$  (dashed line),  $\text{HfNb}(\text{PO}_4)_3$  (red line), and  $\text{ZrNb}(\text{PO}_4)_3$  (blue line).

**Table 1. Activation Energy for Ion Conduction, Lattice Volume, and A Ratio<sup>a</sup> for the NASICON Type Solids**

tetraivalent cation species	sample composition	activation energy ( $\text{kJ mol}^{-1}$ )	lattice volume ( $\text{nm}^3$ )	A ratio ( $\times 10^{-3}$ )
Ti (0.0745 nm)	$\text{Ti}(\text{Nb}_{0.8}\text{W}_{0.2})_{5.0/5.2}(\text{PO}_4)_3$	55.4	1.389	1.25
	$\text{TiNb}(\text{PO}_4)_3$	54.3	1.392	1.24
Hf (0.085 nm)	$\text{HfNb}(\text{PO}_4)_3$	59.9	1.48	1.74
Zr (0.086 nm)	$\text{ZrNb}(\text{PO}_4)_3$	60.1	1.48	1.83

<sup>a</sup> A ratio: the volume ratio of the conducting ion species to the lattice ( $V_{\text{ion}}/V_{\text{lattice}}$ ).

energies are almost the same, whereas the conductivity of  $\text{HfNb}(\text{PO}_4)_3$  is slightly higher than  $\text{ZrNb}(\text{PO}_4)_3$ . The  $E_a$  for ion conduction in these solids may be significantly influenced by the bottleneck size of the conducting pathway; therefore, similar  $E_a$  values were obtained for these solids with the same lattice volume. However, because the conductivity itself is also influenced by the strength of the electrostatic interaction between conducting tetraivalent cations and surrounding  $\text{O}^{2-}$

anions, the interaction for the  $\text{Hf}^{4+}$  ion, with electronegativity of 1.3, should be weaker in comparison to  $\text{Zr}^{4+}$  (electronegativity = 1.4), resulting in ease of migration from the original crystallographic position. In the case of  $\text{TiNb}(\text{PO}_4)_3$ ,  $\text{Ti}^{4+}$  cations migrate smoothly through the bottleneck, because the ionic volume of  $\text{Ti}^{4+}$  is relatively small compared with the lattice volume, which can easily be derived from the A ratio (The A ratio represents the  $V_{\text{ion}}/V_{\text{lattice}}$ , which indicates the relative size of the conducting ion to the bottleneck of the ion-conducting pathway in an indirect sense). However, because the electronegativity of  $\text{Ti}^{4+}$  is 1.5, which is higher than those of  $\text{Zr}^{4+}$  and  $\text{Hf}^{4+}$ , the ion conductivity in  $\text{TiNb}(\text{PO}_4)_3$  is lower than  $\text{ZrNb}(\text{PO}_4)_3$  and  $\text{HfNb}(\text{PO}_4)_3$ . On the other hand, for the  $\text{Ti}(\text{Nb}_{0.8}\text{W}_{0.2})_{5.0/5.2}(\text{PO}_4)_3$  solid, the electrostatic interaction between  $\text{Ti}^{4+}$  and  $\text{O}^{2-}$  should be reduced by the introduction of  $\text{W}^{6+}$ , so that easy migration from the original position is expected. As a result, the  $\text{Ti}(\text{Nb}_{0.8}\text{W}_{0.2})_{5.0/5.2}(\text{PO}_4)_3$  solid exhibits 2.2 times higher  $\text{Ti}^{4+}$  conductivity than  $\text{TiNb}(\text{PO}_4)_3$ , whereas the activation energy is almost equal, because the A ratios of both  $\text{Ti}(\text{Nb}_{0.8}\text{W}_{0.2})_{5.0/5.2}(\text{PO}_4)_3$  and  $\text{TiNb}(\text{PO}_4)_3$  are almost the same.

In conclusion, we have successfully developed pure  $\text{Ti}^{4+}$  ion conducting  $\text{Ti}(\text{Nb}_{0.8}\text{W}_{0.2})_{5.0/5.2}(\text{PO}_4)_3$  without electronic conduction for the first time by strict selection of both the three-dimensional NASICON-type crystal structure and the constituent elements. High  $\text{Ti}^{4+}$  ion conductivity was obtained, similar to that for  $\text{Zr}^{4+}$  and  $\text{Hf}^{4+}$  ions in  $\text{ZrNb}(\text{PO}_4)_3$  and  $\text{HfNb}(\text{PO}_4)_3$ .

**Acknowledgment.** This work was supported by the Industrial Technology Research Grant Program in 2005 (Project ID: 05A18011d) from the New Energy and Industrial Technology Development Organization (NEDO) of Japan.

**Supporting Information Available:** Detailed experimental procedures, XRD patterns of the prepared samples, and the XRD patterns of the electrolyzed sample; result of  $\text{TiNb}(\text{PO}_4)_3$  (PDF). This material is available free of charge via the Internet at <http://pubs.acs.org>.

CM803193K